UNIVERSITY OF CALIFORNIA, SAN DIEGO

Employing metabolic models of *Salmonella* Typhimurium to predict synthetically lethal gene pairs to guide antibiotic discovery

A thesis submitted in partial satisfaction of the requirements for the degree Master of Science

in

Biology

by

Nicole Liu Fong

Committee in charge:

Bernhard Palsson, Chair
Nigel Crawford, Co-Chair
Ella Tour
Karsten Zengler

2012

The thesis of Nicole Liu Fong is approved, and it is acceptable

in quality and form for publication on microfilm and electronically:

_____

_____

_____
Co-Chair

_____
Chair

University of California, San Diego

2012

Dedication

This thesis is dedicated in loving memory of my dear grandmother.

Table of Contents

List of Figures

List of Tables

Acknowledgements

I would like to express my gratitude to my thesis advisor, Dr. Bernhard Palsson for giving me the opportunity to join this lab. I would also like to thank Dr. Nigel Crawford, Dr. Ella Tour, and Dr. Karsten Zengler for taking time out of their busy and hectic schedules to be on my thesis committee.

I would especially like to thank Dr. Pep Charusanti for being an incredible mentor. Thank you so much for your guidance and patience. I really would not be where I am today without you. I appreciate everything that you've done for me and I feel very lucky to have been trained by the prestigious Pep Academy.

I'd also like to thank Joshua Lerman, Mallory Embree, Haythem Latif, Kathy Andrews, Dr. Ramy Aziz, Merve Sahin, Irene Lam, Howard Li, Dongyeon Kim, and DaeHee Lee for their support and insightful conversations. You all deserve free subway lunches and animal crackers for life.

Lastly, I'd like to thank my family and friends for their unwavering support.

ABSTRACT OF THE THESIS

Employing metabolic models of *Salmonella* Typhimurium to predict synthetically lethal gene pairs to guide antibiotic discovery

by

Nicole Liu Fong

Master of Science in Biology

University of California, San Diego, 2012

Professor Bernhard Palsson, Chair

Nigel Crawford, Co-Chair

The growing rates of drug resistant pathogenic bacteria have become a discernible public health crisis, especially in a state in which drug approval rates have dramatically declined. A potential solution to this epidemic is the utilization

of a high-throughput screening method that employs metabolic models to predict new possible drug targets based on synthetic lethality. Here we test the ability of STM_V1.0, a model based on the metabolism of *Salmonella* Typhimurium LT2, to accurately predict synthetic lethal (SL) gene pairs through experimental validation. We also demonstrate a new method to reconcile the model with experimental data in cases where the model predictions lead to false positive results. Results from the generation of the single and double knockouts corresponding to the predicted SL gene pairs confirm that *gltB/gdhA*—one of the four selected gene pairs selected for experimental validation—was indeed synthetically lethal, whereas *sucC/lpdA*, *glyA/serA*, and *ppc/mdh* were not. Hypotheses made by the models successfully explained one of these false positive results, revealing that the overexpression of the *aceBAK* operon was sufficient in rescuing growth in the *ppc* knockout mutant. These results demonstrate the models have the ability to predict synthetic lethality and also to propose testable hypotheses to resolve discrepancies between *in silico* predictions and experimental data.

1. INTRODUCTION

1.1 Antibiotic Resistance

Over the past decade, the world has seen an alarming increase in antibiotic resistant pathogenic bacteria. This spread and rise of resistance can be attributed in part to the misuse of antibiotics in the medical and agricultural field. Recent studies report that physicians were 31% more likely to unnecessarily prescribe antibiotics to patients who expected them compared to those that did not (Ong et al. 2007). The overuse of antibiotics has given bacteria the chance to acquire mutations and overcome these drugs. For example, methicillin-resistant *Staphylococcus aureus* (MRSA) has developed resistance to many classes of antibiotics such as beta-lactams, aminoglycosides, and fluoroquinolones (Holmes et al. 2011). Although new drugs such as Zyvox have been developed to target MRSA, researchers have recently isolated a MRSA strain resistant to this drug (Locke et al. 2011). It is only a matter of time before more strains of MRSA become resistant to this drug too.

Furthermore, a surprising 70% of all manufactured antibiotics in the U.S. are used in agricultural settings, such as in feed additives to fatten and promote faster growth in livestock (Mellon et al. 2001). This exploitation of antibiotics in livestock contributes to the constant selection of drug-resistant bacteria by giving them an opportunity to evolve adaptively via advantageous mutations (Mellon et al. 2001). Reports of foodborne outbreaks in 2000 due to antibiotic-resistant bacteria have increased by more than 300% when compared to 1970 in the

bacteria have increased by more than 300% when compared to 1970 in the United States (Dewall et al. 2011). Of 31 cases of foodborne outbreaks caused by pathogenic bacteria in the United States, 80% of bacteria responsible for the outbreak were resistant to three or more antibiotics, most of which were classified by the World Health Organization as “critically or highly important” to human medicine (Dewall et al. 2011). “Critically or highly important” antimicrobials are classified based on the criteria that they are: the only or one of the few therapies used to treat a severe human disease and used to treat diseases transferred by nonhuman sources (Kennedy et al. 2010). Given this definition of “critically or highly important” antimicrobials, it is frightening that multiple strains of pathogenic bacteria have grown resistant to these antibiotics (Dewall et al. 2011).

As a result of the increasing number of antimicrobial resistant pathogenic strains, the United States has suffered significant financial and detrimental consequences. For instance, outbreaks of *E. coli* result in about 15,000 cases of foodborne illnesses. These outbreaks impose a cost of $ 216-580 million dollars to the US economy every year (Mark et al. 1993). Also, the emergence of these drug-resistant bacteria has become a major health concern considering the fact that bacterial infections are one of the leading causes of death in the elderly and children (Howard et al. 1994). Whether or not this increase in drug-resistance is attributed to overprescription by physicians or misusage by the agricultural

industry, it is clear that society is in dire need for a solution to this epidemic of increasingly resistant pathogens.

Disturbingly, the amount of new antibiotics approved in the United States has significantly decreased, while the numbers of drug-resistant pathogens are on the rise. Sixteen antibiotics were approved in 1983-1987 versus a mere six in 2003-2007 (Boucher et al. 2009). Conventional drug discovery methods involve isolating natural compounds and screening them against multiple pathogens; however, this process is slow, expensive, and inefficient. It takes an average of 12 years for a drug to go from the research lab to the patient at a costly price of $400 million to $1.8 billion (Shirley 2011). Furthermore, only 10% of drugs that begin preclinical testing make it to human testing and of those, only 20% is approved for human usage (Shirley 2011).

One of the problems contributing to this slow rate of drug-development is the screening of which bacterial genes to target. A potential solution to combat this high-cost and time consuming drug discovery method is by utilizing a high-throughput screening system that employs metabolic network reconstructions to identify new bacterial gene targets (Feist et al. 2009).

1.2 Metabolic Network Reconstructions

Metabolic network reconstructions are computationally generated models of organisms that are based on the genes, enzymes, and reactions that

participate in metabolic pathways (Feist et al. 2009). In these computationally generated models, all components known to be involved in metabolism and their interactions are represented within a mathematical stoichiometric matrix in which each metabolite is represented by a column and each reaction is represented by a row (Reed et al. 2006). Appropriate constraints can then be applied to these models to predict phenotype from genotype. These models have proven to be a useful tool for discovering new pathways, targets for therapeutic drugs, and more. For example, the discrepancy between the *in silico* prediction and experimental result of *E. coli* growth on D-malate led to the discovery of the D-malate catabolism pathway (Reed et al. 2006).

1.3 Synthetic Lethal Gene Pairs

Computational simulations using constraint-based analysis of the models allow for the identification of synthetically lethal genes that are essential for growth *in silico*. The identification of synthetic lethal gene pairs is a useful research platform for discovering new combinations of gene targets for drug development. Synthetically lethal gene pairs are genes that can be individually deleted and still give rise to a viable cell; however, when both genes are knocked-out, the cell is non-viable (Kaelin 2005). Models have been successful in identifying synthetically lethal interactions. For example, of the 49 synthetically lethal gene pairs that were tested in yeast, 49% were correct predictions, which is two orders of magnitude higher than expected by chance (Harrison et al.

2007). In addition, models based on cancer metabolism have been employed to identify synthetic lethal gene pairs for combinatorial drug therapy that selectively targets cancer cells and not normal ones (Folger et al. 2011). Based on this, we can also apply this method of identifying synthetic lethal gene pairs for combinatorial drug therapy against pathogenic Enterobacteria, which has not been as aggressively pursued in the field of antibacterial research.

Hypothetically, molecules that target validated synthetic lethal gene pairs in Enterobacteria have the ability to inhibit bacterial growth, and thus are attractive candidates for drug development. The models can predict synthetic lethal interactions between multiple genes, providing insight on synthetic lethal triplicates, quadruplets, and more. The benefits of identifying synthetically lethal interactions through modeling are many. For example, combinational drug therapy based on targeting two or more overlapping pairs of synthetic lethal genes (i.e. two sets of synthetic lethals pairs in which the sets share one gene in common) can minimize the eventual onset of resistance. In theory, this should beneficially delay the development of resistance due to the fact that the pathogen must acquire multiple individual and independent mutations in at least two genes, in order to become resistant. Also, employing genome-scale metabolic models to predict synthetic lethality helps avoid the high-cost and time that would otherwise be spent in constructing all possible single and double-deletion mutants and characterizing each for synthetic lethality. The utilization of metabolically reconstructed models will help speed and aid the process of

discovering new antimicrobials by identifying new potential bacterial drug targets via computational high-throughput screening.

My project is to validate the synthetically lethal gene pairs predicted by the reconstructed metabolic model of *Salmonella* Typhimurium LT2, STM_V1.0, in *Salmonella* Typhimurium 14028s (Thiele and Hyduke et al. 2011). We chose to validate the synthetically lethal gene pairs as predicted by *S.* Typhimurium LT2 in *S.* Typhimurium 14028s because *S.* Typhimurium 14028s would be more applicable for drug targeting due to its virulence (Badie et al. 2007). *S.* Typhimurium LT2 and *S*. Typhimurium 14028s share about 98% of their genomes. The major differences between the two strains can be attributable to two additional prophages, one of which contains two virulence genes, present in 14028s but not in LT2 (Jarvik et al. 2010). Although the discrepancies between the two genomes may also contribute to alternative metabolic pathways in 14028s, which may not be present in the LT2 model, we postulate the differences in 14028s mainly facilitate pathogenesis.

In order to test the ability of the LT2 model to successfully predict synthetic lethality in 14028s, four sets of synthetically lethal gene pairs were selected for experimental validation. The single and double knockouts corresponding to the synthetic lethal gene pairs were generated in *S.* Typhimurium 14028s and characterized by measuring growth rates. The four sets of gene pairs chosen for experimental validation were *gltB*/*gdhA*, *sucC*/*lpdA*, *glyA*/*serA*, and *ppc*/*mdh*.

The first putative synthetically lethal gene pair we tested was *gltB* and *gdhA,* which encode for glutamate synthase and glutamate dehydrogenase. Glutamate synthase and glutamate dehydrogenase are involved in glutamate biosynthesis and both catalyze the reversible conversion of alpha-ketoglutarate into glutamate (Miller et al. 1984). Although a Δ*gltB*Δ*gdhA* double mutant exists in *E. coli* K12 (Dabbs 1982), we wanted to confirm the synthetic lethal prediction in *S.* Typhimurium 14028s, since the double knockout may exhibit a different phenotype specific to each organism.

The second predicted synthetically lethal gene pair selected for experimental validation was *sucC* and *lpdA,* which encode for genes involved in the tricarboxylic acid (TCA) cycle. Succinyl-CoA synthetase, *sucC*, reversibly converts succinyl-coA into succinate (Cunningham et al. 1998). Lipoamide dehydrogenase, *lpdA,* on the other hand is a component of multiple enzyme complexes such as the glycine cleavage system and alpha-ketoglutarate dehydrogenase, which catalyzes the reversible conversion of alpha-ketoglutarate, NAD+, and coenzyme A into succinyl-coA, CO2, and NADH (Douce et al 2011). Together, succinyl-coA synthetase (*sucC*) and lipoamide dehydrogenase (*lpdA*) ultimately convert alpha-ketoglutarate into succinate. We chose to validate this synthetic lethal pair because the relationship between *sucC* and *lpdA* has yet to be characterized in literature.

The next synthetic lethal gene pair that was chosen for validation was serine hydroxymethyltransferase *(glyA)* and phosphoglycerate dehydrogenase

(*serA*). Serine hydroxymethyltransferase is involved in the glycine cleavage system, which converts glycine, NAD+, and water into serine, carbon dioxide, ammonia, NADH, and H+ (Douce et al. 2011). Phosphoglycerate dehydrogenase catalyzes the first committed step in the biosynthesis of serine (Zhao et al. 1996). Previous studies suggest that *serA* and *glyA* are not synthetically lethal in *E. coli* K-12 MG1655 (Orth et al. 2011). However, the synthetic lethal interactions of *serA* and *glyA* have not been investigated and characterized in *S.* Typhimurum 14028s, making the gene pair an interesting candidate for experimental validation.

The last predicted synthetically lethal gene pair selected for *in vivo* validation was phosphophenolpyruvate carboxylase (*ppc*) and malate dehydrogenase (*mdh*). Phosphophenolpyruvate carboxylase converts phosphophenolpyruvate into oxaloacetate and malate dehydrogenase catalyzes the reversible conversion of malate into oxaloacetate (Peng et al. 2004; Sutherland et al. 1985). Since both enzymes are involved in regenerating TCA cycle intermediates, it will then be interesting see if there is a synthetic lethal interaction between these two chosen genes.

Here we demonstrate that STM_V1.0 can correctly predict synthetically lethal gene pairs in *S.* Typhimurium 14028s, which can then possibly be used as gene targets for drug development. We also demonstrate the ability of the models to investigate false predictions, and hypothesize and test possible

compensatory pathways which may provide insight on unknown relationships between genes.

2. MATERIALS AND METHODS

2.1 Prediction of Synthetically Lethal Gene Pairs

The genome scale metabolic model for *Salmonella* Typhimurium LT2 (Thiele and Hyduke et al. 2011) was obtained in sbml format. Synthetic lethal gene pair predictions were performed by computationally inhibiting all pairs of genes in the model. *In silico* growth rates calculated by maximizing flux through the default biomass reaction and values less than $1x10^{-6}$ were defined as no growth.

2.2 Bacterial strains and growth media

2.2.1 Bacterial Strains

Bacterial strains used in this study are summarized in Table 1. *Salmonella* Typhimurium 14028s was a generous gift provided by Fred Heffron at Oregon Health Sciences University.

2.2.2 Growth Media

Strains of *Salmonella* Typhimurium 14028s were cultured at 37°C with magnetic stir bars for aeration in either Luria-Bertani (LB) broth or M9 minimal medium containing 2 g/L glucose, 100 µM $CaCl_2$, 200 mM MgSO4, 13.6 g/L Na_2HPO_4, 6 g/L KH_2PO_4, 1 g/L NaCl, 2 g/L NH_4Cl and 500 µL trace elements. The trace element solution consisted of (per liter): $FeCl_3 \cdot 6H_2O$ (16.67 g), $ZnSO_4 \cdot 7H_2O$ (0.18 g), $CuCl_2 \cdot 2H_2O$ (0.12 g), $MnSO_4 \cdot H_2O$ (0.12 g), $CoCl_2 \cdot 6H_2O$ (0.18 g) and $Na_2EDTA \cdot 2H_2O$ (22.25 g).

Antibiotics were added at the following concentrations: ampicillin at 100 μg/mL, kanamycin at 50 μg/mL, and chloramphenicol at 25 μg/mL.

For complementation analysis of mutants, M9 medium was supplemented with 10 mM of glutamate or 5 mM of glycine, serine, or succinate.

2.3 Plasmid isolation

Overnight cultures containing the appropriate antibiotic were pelleted and plasmid DNA was purified using the QIAprep Spin Miniprep Kit according to the manufacturer's instructions. DNA was quantified and qualified using a NanoDrop ND-1000 Spectrophotometer.

2.4 Construction of knockout strains

Knockouts in *S.* Typhimurium 14028s were generated using the lambda Red recombination system (Datsenko and Wanner 2000). *S.* Typhimurium kanamycin resistance cassettes were generated by PCR using pkD13 as a template with flanking FRT sites and contains 50-nt ends homologous upstream and downstream of the gene of interest. The plasmids pKD46 and pCP20 were used to homologously recombine the kanamycin cassette into the genome and remove the kanamycin resistance marker, respectively. Internal primers specific for each knockout were used to confirm the absence of the gene in the chromosome. PCR products were purified with the QIAGEN PCR clean-up kit.

Overnight cultures were diluted 1:100 into 100 ml of LB media with the appropriate antibiotics and harvested at mid-log phase (OD_{600} ~0.5).

Electrocompetent cells were prepared by pelleting at 4200 rpm for 5 minutes at 4°C, washing twice with ice cold 10% glycerol, and resuspending in residual supernatant. 50 uL of electrocompetent cells were then incubated with 5 uL of plasmid in a 0.2 cm cuvette on ice for five minutes. After electroporation with the Bio-Rad Gene Pulser at 2.5 kV, cells were immediately recovered in 300 uL of SOC media at the appropriate temperature for 1 1/2 hours. Positive transformants were then selected on LB agar with the appropriate antibiotic. The final concentrations of antibiotics for selective growth are listed above.

2.5 Phenotypic Characterization

2.5.1 Complementation

Auxotrophic strains were cultured in LB medium overnight, spun down and washed twice with M9 medium, and used to inoculate 20 mL of M9 medium supplemented with 10 mM glutamate or 5 mM of serine, glycine, or succinate.

2.5.2 Growth rate and glucose uptake rates

Strains were cultured in LB media overnight, spun down and washed twice in M9 glucose, and used to inoculate 25 mL flasks containing 10 mL of M9 glucose. Cultures were aerated and agitated by a magnetic stirring bar at 37°C in an air incubator. The next day, cultures were inoculated into 250 mL Erlenmeyer flasks containing 100 mL of M9 glucose in triplicate at an initial OD_{600} of 0.05. The flasks were then transferred to a 37°C water bath with continuous agitation as described above.

Cell growth was monitored by measuring the optical density at 600 nm (OD_{600}) with a Biomate 3 series spectrophotometer. The optical density of each sample was recorded every 30 minutes and culture media was filtered through a 0.22uM membrane. The glucose concentration in the medium was assessed using refractive index detection by high performance liquid chromatography with a Bio-Rad Aminex HPX87-H ion exclusion column (injection volume, 10 uL) and 5 mM H_2SO_4 as the mobile phase (.5ml/min, 30°C).

Biomass was measured in triplicate 50 mL cultures of WT at different cell densities in LB media. Cells were spun down in 50 mL falcon tubes and allowed to dry overnight in a 60°C incubator and weighed. Using this data, we calculated a conversion of 0.41 gDW/L per unit OD (R^2 = 0.94). This value was used to calculate glucose uptake rates in Table 3.

2.6 Overexpression

2.6.1 Model guided rescue of a *ppc* mutant

For both models (STM_V1.0 and i*JO*1366) the total network flux to grow at a rate of 0.1 hr^{-1} was minimized (Thiele and Hyudke et al. 2011; Orth et al. 2011). Specifically, the reaction network was made irreversible and the objective was to minimize the sum of all fluxes as previously described (Lewis et al. 2010). A priority score was assigned to capture adverse network effects of double knockouts that do not show a decrease in growth rate as metabolic models do not account for the total cost of protein synthesis. The priority score was defined as: $Min_{\text{flux of double knockout}} - Max(Min_{\text{flux with knockout1}}, Min_{\text{flux with knockout2}})$.

2.6.2 Construction of pS1988 conferring *Cam*^{R}

The ampicillin resistance gene of pASK-IBA33+ (IBA, Goettingen, Germany) was replaced with the chloramphenicol resistance gene of pACBSR. Primers were used to add AgeI and BlpI restriction sites to the chloramphenicol resistance gene (*cat*) of pACBSR and the backbone of pASK-IBA33+ excluding the ampicillin resistance gene via PCR. PCR was performed using the Phusion DNA polymerase from New England BioLabs. The resulting PCR products were purified from a 1% agarose gel using the QIAGEN QIAquick Gel Extraction Kit according to the manufacturer's instructions. The two purified PCR fragments were then digested with AgeI and BlpI at 37°C for 4 hours and ligated with T4 DNA ligase at 16°C overnight. The ligated products were then transformed into TOP10 cells by heat-shock at 42°C, recovered in SOC media, and plated on selective chloramphenicol agar plates. Successful transformants were cultured in LB media with chloramphenicol overnight, plasmid DNA was isolated, and PCR was used to confirm the isolation of the desired plasmid. All restriction enzymes and ligase were obtained from New England BioLabs.

2.6.3 Construction of pS6, pS7, pS8, pS10

The genes, *aceA*, *aceBA*, *aceK*, and *aceBAK* were amplified by PCR using *S.* Typhimurium 14028s genomic DNA as a template. The genes, *aceA*, *aceBAK*, and *aceBA* were cloned into pASK-IBA33+ and *aceK* was cloned into pASK1988, yielding pS6, pS7, pS8, and pS10, respectively.

2.6.4 Induction

Overnight strains cultured in LB medium with the appropriate antibiotics were used to inoculate two 250 mL Erlenmeyer flasks containing 20 mL of LB medium at an initial OD_{600} of 0.05 at 37°C. One flask was induced at mid-log phase (OD600 ~0.5) with anhydrotetracycline (ATc) at a final concentration of 100 ng/mL. Both flasks were then cultured for an additional 3 hours, after which were spun down and washed twice with M9 medium. The washed cells were then each used to inoculate 250 mL Erlenmeyer flasks containing 100 mL of M9 medium with or without inducer in triplicate. The six flasks were then placed in a 37°C water bath and optical density was measured periodically.

2.7 Whole genome sequencing

2.7.1 Library construction for whole genome sequencing

Genomic DNA libraries were prepared using the Nextera DNA Sample Prep Kit (Illumina-compatible). Genomic DNA was tagmented using the 5X HMW Nextera Reaction Buffer and purified with the QIAGEN MinElute PCR purification Kit according to the manufacter's instructions. After the addition of bPCR-compatible sites and library enrichment, the DNA library was purified with Agencourt® AMPure® XP beads (0.7X). The quality and fragment distribution of the library was verified by using the Agilent 2100 Bioanalyzer.

2.7.2 Library validation and sequencing

1 uL of the purified library was cloned into the pCR-Blunt II-TOPO® vector (Invitrogen) and then transformed into One Shot TOP10 Chemically Competent Cells (Invitrogen). Successful transformants were selected on LB plates containing 50 μg/ml of kanamycin at 37°C overnight. The inserts of the transformants were amplified via PCR using M13-FOR and M13-REV primers and sequenced to ensure proper incorporation of barcoded adaptors. Validated libraries were then run on the Illumina MiSeq platform.

2.7.3 Data analysis

Reads were mapped to the reference genome (NCBI accession number: NC_016856 and NC_016856) via Breseq, which was developed by the Barrick lab of The University of Texas at Austin.

3. RESULTS

3.1 Synthetic Lethal Gene Pair Predictions

GltB/GdhA was confirmed experimentally to be a synthetic lethal gene pair, but LpdA/SucC, SerA/GlyA, and ppc/mdh were false positive model predictions

To investigate the ability of the models to correctly predict synthetic lethality, we constructed four sets of double knockouts and eight single knockout mutants in *S.* Typhimurium 14028s that corresponded to predicted synthetic lethal pairs (Table 1). The four pairs generated are *gltB*/*gdhA*, *lpdA*/*sucC*, *glyA*/*serA*, and *ppc*/*mdh*. The gene pairs—*gltB*/*gdhA*, *glyA*/*serA*, and *ppc*/*mdh*—were predicted to be synthetically lethal in M9 glucose minimal media (M9), whereas *lpdA*/*sucC* was predicted to be synthetically lethal in Luria-Bertani media (LB) (Table 2).

3.1.1 *gltB/gdhA*

We experimentally constructed a *gltB*/*gdhA* double knockout and confirmed that it is a synthetic lethal pair in M9 media, as predicted by the model. We successfully generated *gltB* and *gdhA* single knockouts and the *gltB*/*gdhA* double knockout in LB media. *gltB* and *gdhA* single mutants can grow in M9 media due to the fact that the other gene can compensate for the loss of the other. However, the double knockout is auxotrophic for glutamate in M9 media, since the cell cannot synthesize this amino acid. When the two single knockouts

were switched from LB to M9 media, both were still able to grow; however, the double knockout did not (Figure 3A). The *gdhA* and *gltB* single mutants grew slightly slower than WT in M9 media at a rate of 0.77±0.01 hr^{-1} and 0.63±0.01 hr^{-1} versus 0.86±0.02 hr^{-1}. When the Δ*gltB*Δ*gdhA* double mutant was supplemented with 10 mM of glutamate, growth was restored at a rate of 0.74±0.03 hr^{-1}. Furthermore, glucose uptake rates for the *gdhA* and *gltB* single mutants calculated were 14±1.5 mmol/gDW/hr and 7.4±5.3 mmol/gDW/hr, whereas the Δ*gltB*Δ*gdhA* double mutant and WT exhibited corresponding glucose uptake rates of 24±3.6 mmol/gDW/hr and 15±0.41 mmol/gDW/hr. The glucose uptake rates for the *gdhA* single mutant and WT were similar, whereas the glucose uptake rate decreased by half in the *gltB* single mutant. Also, when supplemented with 10 mM glutamate, the Δ*gltB*Δ*gdhA* double mutant exhibited a 1.6 fold increase in glucose uptake rate as compared to WT (Table 4).

3.1.2 *lpdA/sucC*

The second predicted synthetically lethal gene pair that we chose to experimentally validate in S. Typhimurium 14028s was *lpdA*/*sucC*, which was predicted to be synthetically lethal in LB medium. We experimentally constructed the two single knockouts and the double knockout and found that *lpdA* and *sucC* are not synthetically lethal gene pairs in LB media as predicted by the models. Although the loss of either gene does not prohibit growth in LB media, loss of both genes does not prohibit growth either. The *sucC* single knockout grew at a rate of 1.52±0.04 hr^{-1} , similar to WT. The Δ*lpdA*Δ*sucC* double knockout and *lpdA*

mutant however, grow about twice as slow as WT in LB medium: 0.65±0.02 hr^{-1} and 0.76±0.01 hr^{-1} vs 1.54±0.05 hr^{-1} (Figure 3B). In addition, the *lpd* and Δ*lpdA*Δ*sucC* mutants form tiny pin-prick colonies on LB plates, suggesting a growth defect.

3.1.3 *serA/glyA*

Experimental construction of a Δ*serA*Δ*glyA* double knockout revealed that it is not a synthetic lethal pair. The generated *serA* and *glyA* single knockout mutants that were generated in LB media were found to be singly essential in M9 media. The *serA* and *glyA* mutants were unable to grow in M9 media unless supplemented with serine or glycine, respectively. When supplemented with 5 mM of serine or glycine, the growth rates of the *serA* and *glyA* single mutants were 0.78±0.02 hr^{-1} and 0.61±0.01 hr^{-1}, corresponding to a 1.1-fold and 1.4-fold decrease in growth rate compared to WT (Figure 3C). When supplemented with 5 mM of serine, glucose uptake rates in the *serA* mutant was 6.4±3.0 mmol/gDW/hr, about almost half the rate of WT, 15±0.41 mmol/gDW/hr (Table 4). The *glyA* mutant exhibited a glucose uptake rate of 4.0±5.5 mmol/gdw/hr. The Δ*serA*Δ*glyA* double mutant was also unable to grow when switched from LB to M9 medium, unless supplemented with both serine and glycine. Interestingly, even when supplemented with 5 mM serine and glycine, full WT-like growth was not restored in the double mutant, which exhibited a growth rate of only 0.29±0.01 hr^{-1} and a glucose uptake rate of 6.9±1.5 mmol/gDW/hr.

3.1.4 *ppc/mdh*

We experimentally constructed a Δ*ppc*Δ*mdh* double mutant and discovered that it is not a synthetic lethal pair. The *mdh* mutant was viable in M9 medium and grew 1.7x slower than WT in M9 media at a growth rate of 0.49±0.01 hr^{-1} (Figure 3D). The glucose uptake rate calculated for the *mdh* mutant in M9 medium was 10±2.9 mmol/gDW/hr (Table 4). The *ppc* knockout mutant, on the other hand, was found to be nonviable in M9 media. Supplementation of M9 media with 5 mM of succinate restored growth in the *ppc* mutant at a rate of 0.87±0.01 hr^{-1}, similar to that of WT. The glucose uptake rate calculated for the supplemented *ppc* mutant (14±6.2 mmol/gDW/hr) was also similar to WT (15±0.41 mmol/gDW/hr). Succinate supplementation also slightly increased the growth rate of the *mdh* mutant to 0.74±0.04 hr^{-1} and decreased the glucose uptake rate to 4.7±1.5 mmol/gDW/hr. Succinate supplementation was unable to rescue the Δ*ppc*Δ*mdh* double mutant. Since the *ppc* single knockout was found to be singly essential, it is then not surprising that the Δ*ppc*Δ*mdh* double mutant was also nonviable in M9 media. Despite the fact that the Δ*ppc*Δ*mdh* double mutant exhibits lethality, this gene pair is not synthetically lethal because the *ppc* single knockout is non-viable.

3.2 Rescuing growth in the *ppc* mutant

3.2.1 Model guided rescue of the *ppc* mutant

Both STM_V1.0 and i*JO*1366 (genome-scale metabolic model of *E. coli)* were utilized to predict which genes when overexpressed might rescue the *ppc*

mutant (Orth et al. 2011). We hypothesized that overexpressing genes that are computationally essential in the *ppc* mutant will restore growth. Also, as models do not take into account the total cost of protein synthesis, we calculated the total minimal flux for all possible single knockout mutants and then compared it to the total minimal flux of all possible *ppc* double knockout mutants. Double mutants that had a significant increase in total minimal flux were investigated as possible candidates to explain why the model did not correctly predict that the *ppc* single knockout is non-viable (Table 4 and 5).

The top candidate of interest based on both models was isocitrate lyase, encoded by *aceA*. In STM_V1.0, *aceA* is essential in the *ppc* mutant, whereas in i*JO*1366, the minimal sum of flux showed a large increase, indicating *aceA's* importance in the *ppc* mutant. Isocitrate lyase is part of the *ace* operon, *aceBAK*, which encodes the genes necessary for the glyoxylate shunt. This shunt redirects flux from the latter steps of the TCA cycle and helps regenerate the TCA cycle intermediates, thus bypassing two decarboxylation steps (Figure 6). Interestingly, supplementation of M9 media with the intermediates of the glyoxylate shunt (glyoxylate, malate, and succinate) restores growth in the *ppc* mutant, which provided us with further incentive to investigate the relationship between the *ppc* knockout and the glyoxylate shunt genes (Table 6).

3.2.2 Knocking out iclR in the ppc mutant rescues growth

A *ppc* mutant is unable to convert phosphophenolpyruvate (PEP) into oxaloacetate (Peng et al. 2004). This may lead to an accumulation of PEP within

the cell. If this holds true and excess PEP is converted into pyruvate, this may activate IclR and inhibit transcription of the glyoxylate shunt genes (Lorca et al. 2007). One can then theorize if the *ppc* mutant is unable to grow due to the inhibition of glyoxylate shunt genes, then a Δ*ppc*Δ*iclR* double mutant that allows for expression of the glyoxylate shunt genes is viable. When we generated the Δ*ppc*Δ*iclR* double mutant, growth was restored in the double mutant (0.45±0.01 hr^{-1}) as predicted at half the rate of WT (0.87±0.01 hr^{-1}) in glucose minimal media (Figure 8). This data further suggests that the glyoxylate shunt genes may play a role in *ppc's* essentiality in M9 medium.

3.2.3 Toxicity of anhydrotetracycline

In order to attribute restoration of growth in the *ppc* mutant solely to the glyoxylate shunt genes, we chose to overexpress the *aceBAK* operon on the pASK-IBA33+ expression vector. pASK-IBA33+ contains a tetracycline inducible promoter and is most optimal for expression in M9 medium. Expression plasmids that utilize other promoters are not as efficient for expression in M9 medium. For example, studies have shown that induction of arabinose and lactose inducible promoters can be repressed due to the glucose present in M9 media (Lee et al. 2011). Vectors with a tetracycline inducible promoter, however, are not susceptible to this repression.

Firstly, we investigated whether anhydrotetracycline (ATc), the molecule used to induce expression of the genes, was toxic to *S.* Typhimurium and determined the optimal concentration for induction. Although ATc is a

degradation product of tetracycline, high concentrations of ATc are lethal to growth (Ehrt et al. 2005). Low concentrations of ATc such as 10 ng/mL, 40 ng/mL, and 100 ng/mL slows growth, however, are not toxic to the cell (Figure 9). Although 200 ng/mL of ATc is not toxic to *S.* Typhimurium 14028s, this concentration of inducer delayed growth. We determined that the concentration of induction at 100 ng/mL most optimally expresses protein without prohibiting growth. Although the manufacturer recommends protein induction at 200 ng/mL, based on our growth curve data, we decided that 100 ng/mL would be most optimal for protein expression and rescuing growth in our *ppc* mutant.

3.2.4 Simultaneous expression of *aceBA* and *aceK* from two separate plasmids can rescue growth in the *ppc* mutant, but overexpression of *aceA*, *aceBA*, *aceK*, and *aceBAK* cannot.

After determining the optimal concentration of inducer, we overexpressed *aceBA* and *aceK* on separate expression plasmids. The *ace* operon was split and expressed on two separate expression vectors due to the presence of a 183 bp intergenic region between *aceA* and *aceK*. Through cloning and PCR, we replaced the ampicillin resistance gene of pASK-IBA33+ with a chloramphenicol resistance gene, yielding pS1988 (Figure 10). *aceBA* and *aceK* was then cloned into pASK-IBA33+ and pS1988, yielding pS8 and pS10, respectively, and transformed into the *ppc* mutant, *ppc*(pS8+pS10*).* Simultaneous expression of *aceBA* and *aceK* rescued growth in the *ppc* mutant. When expression of these two genes were induced at 100 ng/mL of ATc in M9 medium, growth was

restored at half the rate of WT (Figure 11). Growth in the *ppc*(pS8+pS10*)* mutant was also restored on M9 plates with 100 ng/mL of ATc as well (Figure 12). Furthermore, the *ppc*(pS8+pS10) mutant was cured on LB plates with or without either ampicillin or chloramphenicol. Mutants that lost either plasmid were unable to grow when restreaked onto M9 plates with ATc, indicating that maintenance of both plasmids are necessary to rescue growth in the *ppc* mutant.

Next, we investigated whether expression of the entire operon as a whole or single expression of the genes was sufficient to rescue growth in the *ppc* mutant. Overexpression of the entire operon on a single expression vector did not rescue growth in the *ppc* mutant. In addition, a *ppc* mutant overexpressing *aceA* was nonviable in M9 medium, indicating that *aceA* cannot singly rescue growth in the *ppc* mutant. pS8 (*aceBA*) was transformed into the *ppc* mutant and selected on LB ampicillin plates. Successful transformants were restreaked onto M9 plates with and without 100 ng/mL of ATc. After 14 days, colonies failed to grow on both plates, suggesting that overexpression of *aceBA* cannot restore growth in the *ppc* mutant. After transformation of pS10 (*aceK)* into the *ppc* mutant, colonies were unable to grow on M9 plates with or without inducer. This indicates that *aceK* also cannot solely rescue the *ppc* mutant and infers that only the simultaneous overexpression of *aceBA* and *aceK* on two separate plasmids can growth rescue in the *ppc* mutant in M9 media.

3.2.5 Resequencing of ppc(pS8+pS10) shows no additional mutations

Lastly, we resequenced the genome of the *ppc* mutant using Illumina technology to confirm that rescued growth was solely due to expression of the

glyoxylate shunt genes and not spontaneous mutations in other parts of the genome. The sequencing data generated mapped 99.6% of the reads to the reference genome and identified 21 possible mutations (Table 7). After close re-examination, Sanger sequencing confirmed that these putative mutations were simply reference errors.

4. DISCUSSION

Employing STM_V1.0 yielded a number of synthetic lethal gene pair predictions, four of which were then experimentally tested through the construction of the corresponding four double knockouts and their associated single knockouts. Phenotypic characterization of these mutants revealed that one of four predicted SL interactions were correct, whereas three out of four were not. The investigation of the inconsistencies between *in silico* predictions and experimental data—particularly in the *ppc* mutant—show that the models can formulate testable hypothesis about false positive predictions to reconcile these discrepancies.

One out of four synthetic lethal gene pairs were accurately predicted by STM_V1.0. Three of these four were not synthetic lethal gene pairs. For two of these pairs, one or both of the genes were singly essential. For the last pair (*sucC*/*lpdA*), it is hypothesized that there is an alternative pathway that compensates for the loss of the two genes that was not included in model. Despite this, we still successfully utilized the models to probe why one of these genes was singly essential, demonstrating that the models can also be utilized to investigate false predictions and fill gaps. In order to increase the accuracy of these predictions, this type of model curation is necessary and beneficiary.

4.1 Gene pairs submitted to AMRI as targets for small molecule-screening

The gene pair, *gltB*/*gdhA* proved to be synthetically lethal as predicted by the models. Because growth was restored in the generated *gltB/gdhA* double mutant to almost WT-like rates with glutamate supplementation, this gene pair was deemed as an unattractive target for drug screening. Although *ppc/mdh*, *lpdA/sucC*, and *glyA/serA*, are not synthetically lethal, the loss of both genes in *S.* Typhimurium 14028s results in reduced growth. Even with supplementation, the growth rates of each double knockout were significantly lower than WT ($P < 0.001$). Due to these growth defects, these gene pairs were submitted to Albany Molecular Research, Inc (AMRI) for virtual and high-throughput screening.

4.2 Phosphophenolpyruvate carboxylase, *ppc,* is a singly essential gene in glucose minimal media

Previous studies suggest that the *ppc* mutant is singly essential in glucose minimal media due to failure of regenerating oxaloacetate, which would hypothetically prevent carbon replenishment of the TCA cycle (Luinenburg 1993). However, this is inconsistent with our findings since supplementation of glucose minimal media with oxaloacetate fails to rescue growth in the *ppc* mutant. This may be due to inefficient transport of oxaloacetate into the cell or suggests that another mechanism may contribute to lethality in the *ppc* mutant. In order to

investigate why *ppc* is singly essential, we employed the *E. coli* metabolic model iJO1366 (Orth et al. 2011) and the *Salmonella* Typhimurium LT2 metabolic model (Thiele and Hyduke et al. 2011) to search for candidate compensatory pathways. All models identified flux through *aceA* as crucial in the *ppc* mutant, which led us to investigate the role of the *aceBAK* operon in the *ppc* mutant. Previous studies have noted increased flux through the glyoxylate shunt in an adaptively evolved *E. coli ppc* mutant (Fong et al. 2006). However, this study also observed decreased flux through pathways involved with succinate dehydrogenase and does not directly illustrate the relationship between *ppc* and the glyoxylate shunt (Fong et al. 2006). Our results suggest that the overexpression of the glyoxylate shunt genes is sufficient in rescuing growth within the *ppc* mutant, as predicted by the models. One possible explanation may be that as a result of knocking out *ppc,* pyruvate accumulates within the cell and activates IclR, isocitrate lyase regulator, which prevents transcription of *aceBAK*—the glyoxylate shunt genes (Lorca et al. 2007). Since the *ppc* mutant cannot regenerate the intermediates of the TCA cycle, the expression of *aceBAK* may be important for renewing these intermediates through bypassing two decarboxylation reactions, which ultimately prevents the loss of two carbons. This may explain why *ppc* is a non-essential gene in the model.

4.3 The intergenic region between *aceA* and *aceK*

Expression of the *aceBAK* operon must occur on two separate plasmids in order to rescue the *ppc* mutant. The *aceBAK* operon encodes for the genes in the

glyoxylate bypass: *aceB* and *aceA* play a role in ultimately converting isocitrate to succinate and malate, whereas *aceK* controls carbon flux between the TCA cycle and the glyoxylate cycle (Cortay et al. 1988). A 183 bp intergenic region exists between *aceA* and *aceK*, which may contribute to "inefficient translation or premature transcription termination" of *aceK (*Chung et al. 1993*;* Cozzone et al. 2005*).* Restoration of growth was not observed in the *ppc* mutant during the overexpression of the entire *aceBAK* operon from a single expression vector. However, when this intergenic region is excluded and *aceBA* and *aceK* are expressed on separate expression plasmids, the *ppc* mutant is viable. These results support the possibility that the intergenic region may interfere with translation or transcription of *aceK*. Interestingly, *aceK* acts as both a phosphorylase and kinase, which respectively activate and inactivate isocitrate dehydrogenase, an enzyme of the TCA cycle (Borthwick et al. 1984). When isocitrate dehydrogenase is activated by *aceK*, this forces flux through the latter steps of the TCA cycle, and diverts flux from the glyoxylate shunt (McKee et al. 1989). However, when isocitrate dehydrogenase is inactivated, isocitrate is diverted from the TCA cycle to the glyoxylate shunt and ultimately converted into succinate and malate (McKee et al. 1989). Due to *aceK's* significant role in controlling flux between these two cycles, it is no wonder that efficient translation of *aceK* is necessary for rescue in the *ppc* mutant. Future studies must be conducted in order to investigate the exact role that this intergenic region plays *in vivo*.

4.4 Conclusion

The increasing prevalence of antibiotic resistant bacteria and dramatic decline of newly approved antibiotic drugs threatens our society. For example, one strain of methicillin-resistant *Staphylococcus aureus* (MRSA) has an alarming 50% mortality rate in hospital patients and has developed resistance to almost all antibiotic drugs (Holmes et al. 2011). It will not be long before MRSA develops resistance to the remaining antibiotics. In order to combat the rapid rise in harmful antibiotic resistant pathogens, a more efficient method of discovering and developing antibiotic drugs must be utilized. Using metabolically reconstructed models could help speed and aid the process of discovering new antibiotics by identifying new potential bacterial drug targets via computational high-throughput screening.

Genome-scale metabolic models are reliable tools for driving biological discovery and have proven their value through various applications, such as metabolic engineering of microorganisms for production of chemicals and materials, understanding cellular metabolism, and more (Sohn et al. 2012). Here we have tested the ability of the models to predict synthetic lethal gene pairs and demonstrate a new method to explain false positive predictions as well. Calculations have been made for the false positive predictions, *serA* and *glyA*. Possible compensatory pathways to be investigated in the future are listed in Table 8 and 9. Many more false positive predictions remain within the model. Investigating these false positive predictions and their compensatory pathways

can uncover previously unknown relationships between genes. There is a strong need for model refinement to fix these false predictions, which will in turn will lead to more accurate predictions of synthetic lethal gene pairs for drug target identification.

Table 1: List of strains and plasmids used in this study

Strain or Plasmid	Relevant Characteristics	Source and/or reference
Strains		
Salmonella Typhimurium 14028s	Wild-type	Heffron[a]
	Δ*serA*	This study
	Δ*glyA*	This study
	Δ*serA*Δ*glyA*	This study
	Δ*gltB*	This study
	Δ*gdhA*	This study
	Δ*gltB*Δ*gdhA*	This study
	Δ*ppc*	This study
	Δ*mdh*	This study
	Δ*ppc*Δ*mdh*	This study
	Δ*sucC*	This study
	Δ*lpd*	This study
	Δ*sucC*Δ*lpd*	This study
	Δ*ppc*(pS8+pS10)	This study
	Δ*ppc*Δ*iclR*	This study
Plasmids		
pkD13	Used as template for generation of kanamycin cassette	Datsenko
pkD46	Temperature sensitive plasmid containing lambda-Red recombination gene under an arabinose-inducible promoter	Datsenko
pCP20	Encodes FLP recombinase	Datsenko
pASK-IBA33+	Expression plasmid containing a tetracycline inducible promoter; Amp^R	IBA
pS1988	Derivative of pASK-IBA33+ containing Cam^R	This study
pS6	pASK-IBA33+ expressing AceA of *S.* Typhimurium 14028s	This study
pS7	pASK-IBA33+ expressing AceBAK of *S.* Typhimurium 14028s	This study
pS8	pASK-IBA33+ expressing AceBA of *S.* Typhimurium 14028s	This study
pS10	pS1988 expressing AceK of *S.* Typhimurium 14028s	This study

[a] Fred Heffron at Oregon Health Sciences University

Amp^R and Cam^R indicate resistance to ampicillin and chloramphenicol, respectively.

Table 2: List of the synthetic lethal gene pairs predicted in STM_V1.0 that were chosen for experimental validation.

Synthetic Lethal Gene Pairs		
	Media	Predicted to be lethal in STM_V1.0 or *i*JO1366*?
Gene Pairs		
gltB/gdhA	M9 only	Yes/Yes
lpdA/sucC	LB	Yes/No
glyA/serA	M9 only	Yes/Yes
ppc/mdh	M9 only	Yes/No

**i*JO1366 is a model of *E. coli* metabolism (Orth et al 2011)

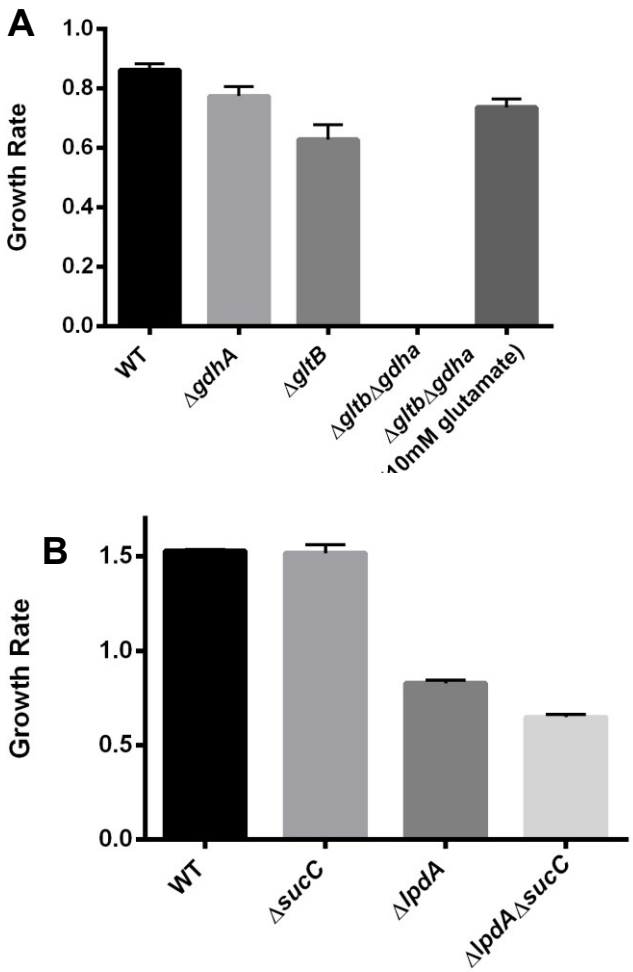

Figure 1A-D: Growth rates of constructed single and double knockout mutants. Mutants were grown in either (A, C, D) glucose minimal media or (B) LB media. Additional supplementation of media was added as noted in parenthesis. Error bars represent standard deviation amongst triplicates.

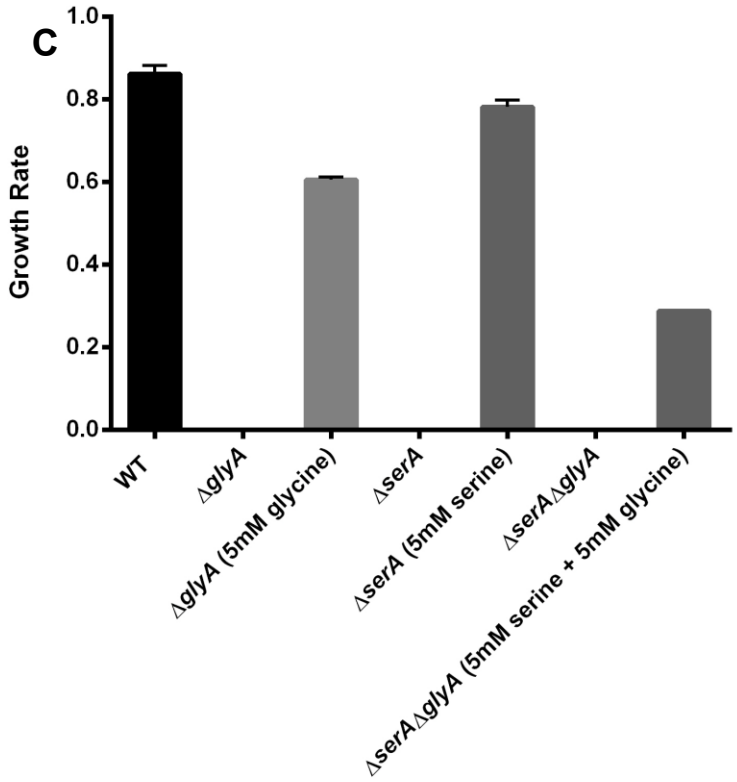

Figure 1A-D continued: Growth rates of constructed single and double knockout mutants.

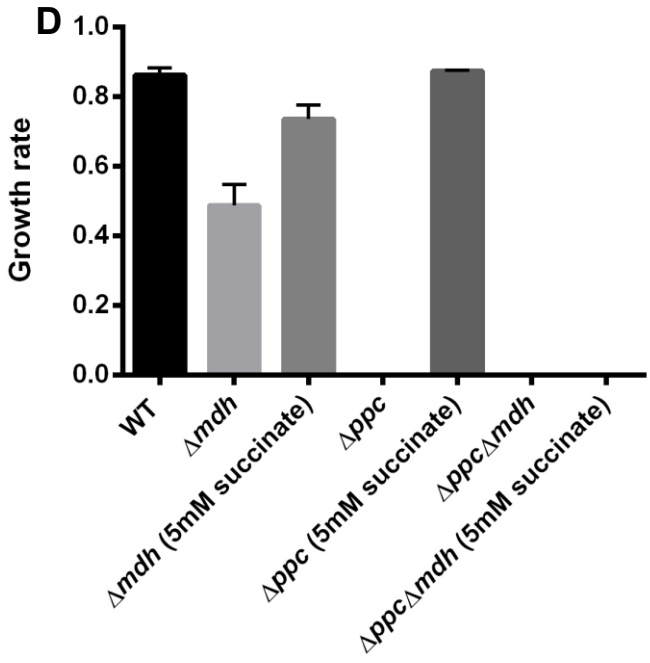

Figure 1A-D continued: Growth rates of constructed single and double knockout mutants.

Table 3: Glucose uptake rates of the constructed mutants.
Average glucose uptake rates (Avg. G.U.R.) calculated for mutants in glucose minimal media. The standard deviations (S.D.) are representative of biological triplicates.

	WT	*ΔgltB*	*ΔgdhA*	*ΔgltBΔ gdhA*[a]	*ΔglyA*[b]	*ΔserA*[c]	*ΔglyA ΔserA*[d]	*Δmdh*	*Δmdh*[e]	*Δppc*[e]
Avg. G.U.R*	15	7.4	14	24	4	6.4	6.9	10	4.7	14
S.D.*	0.41	5.3	1.5	3.6	5.5	3	1.5	2.9	1.5	6.2

*Units are in mmol/gDW/hr (G.U.R. calculations were performed using 0.41 gDW/L per unit OD)
*gDW: grams dry weight
[a] Supplemented with 10 mM of glutamate
[b] Supplemented with 5 mM of glycine
[c] Supplemented with 5 mM of serine
[d] Supplemented with 5 mM of glycine and serine
[e] Supplemented with 5 mM of succinate

Table 4: Genes crucial to the *ppc* mutant as predicted by *i*JO1366.

Gene1	Gene2	Minimal Flux of Gene1 KO	Minimal Flux of Gene2 KO	Minimal Flux of Double KO	Priority Score (Difference in Total Minimal Flux)
ppc	*aceA**	89.59306086	89.43707813	112.982987	23.38992615
ppc	*sdhC*	89.59306086	91.51499808	114.1783407	22.6633426
ppc	*sdhB*	89.59306086	91.51499808	114.1783407	22.6633426
ppc	*sdhD*	89.59306086	91.51499808	114.1783407	22.6633426
ppc	*sdhA*	89.59306086	91.51499808	114.1783407	22.6633426
ppc	*atpA*	89.59306086	150.561861	156.4455432	5.8836822
ppc	*atpH*	89.59306086	150.561861	156.4455432	5.8836822
ppc	*atpF*	89.59306086	150.561861	156.4455432	5.8836822
ppc	*atpE*	89.59306086	150.561861	156.4455432	5.8836822
ppc	*atpC*	89.59306086	150.561861	156.4455432	5.8836822
ppc	*atpD*	89.59306086	150.561861	156.4455432	5.8836822
ppc	*atpG*	89.59306086	150.561861	156.4455432	5.8836822
ppc	*atpB*	89.59306086	150.561861	156.4455432	5.8836822

**aceA* was investigated

Table 5: Newly essential genes specific to the *ppc* mutant as predicted by STM_V1.0.

KEGG[a] gene accession number	Gene Name
STM0733	*sdhD*
STM0734	*sdhA*
STM3359	*mdh*
STM0732	*sdhC*
STM0735	*sdhB*
STM4183	*aceB**
STM4184	*aceA**

[a]Kyoto Encyclopedia of Genes and Genomes

**aceB* and *aceA* were investigated

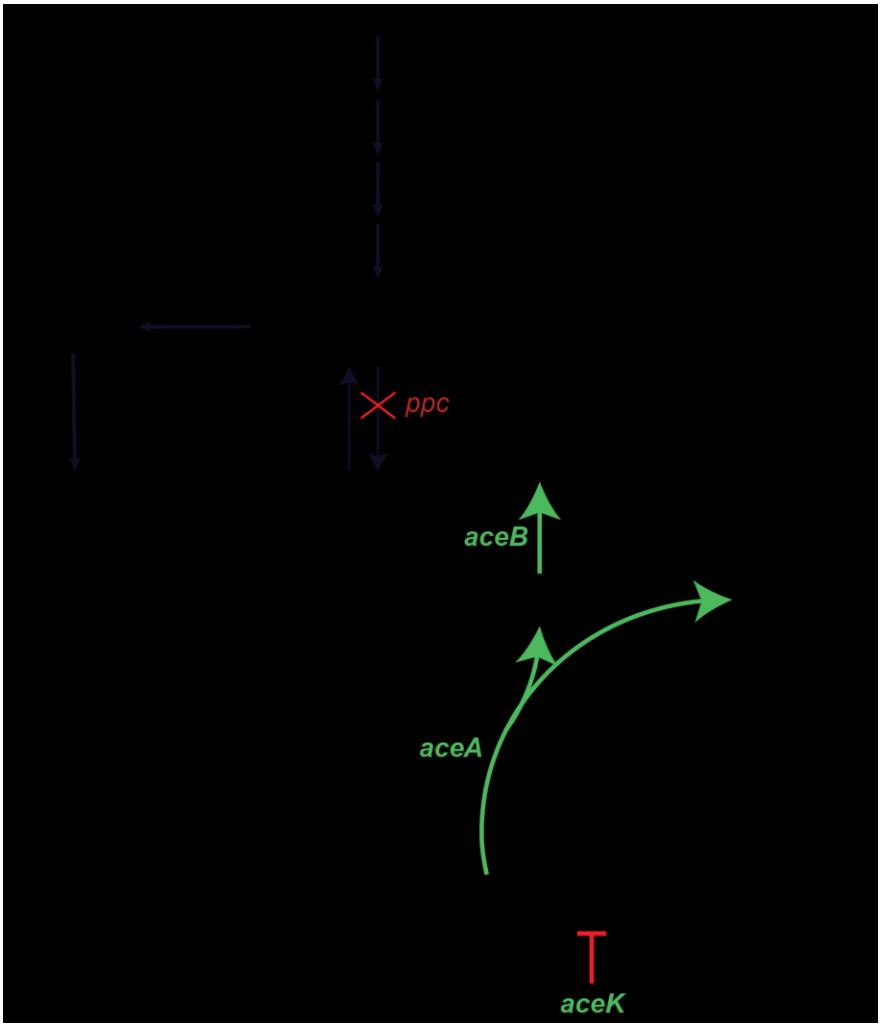

Figure 2: Metabolic pathways in the *ppc* mutant. Reactions and genes in green represent the glyoxylate shunt. (T) represents inhibition.

Table 6: Supplementation of glucose minimal media and its effect on growth in WT and the *ppc* mutant.

	Ace-tate	Pyru-vate	Succ-inate	Fum-arate	Cit-rat e	Mal-ate	Glyox-ylate	Oxalo-acetate	Isoci-trate	Glucose only
WT	G	G	G	G	G	G	G	G	G	G
Δppc	NG	NG	G	G	NG	G	G	NG	NG	NG

G indicates growth, whereas NG indicates no growth. Each metabolite was added to glucose minimal media to a final concentration of 10 mM.

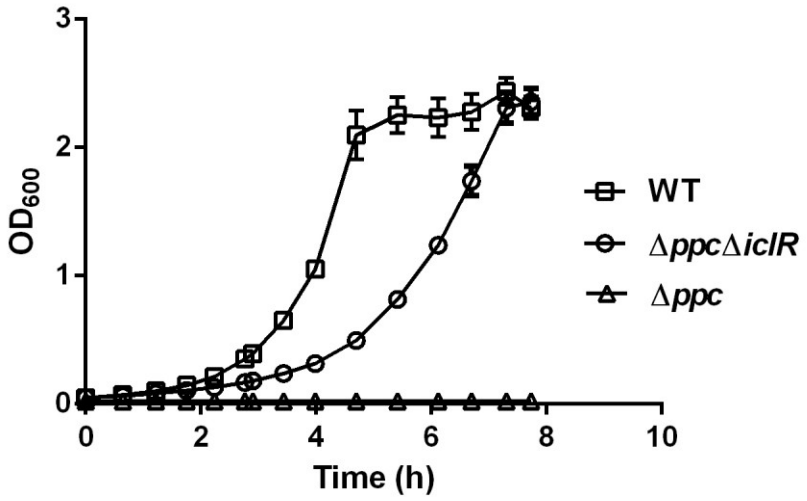

Figure 3: Growth curves of WT, Δ*ppc*Δ*iclR*, and Δ*ppc*. Bacteria were grown in glucose minimal media and cell density was measured over time.

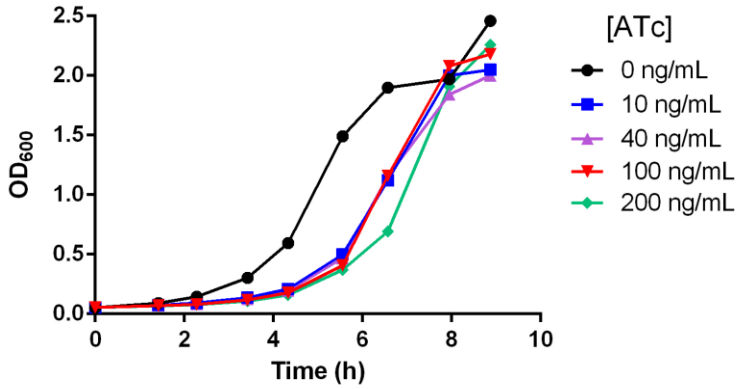

Figure 4: Effect of ATc on the growth of *S.* Typhimurium 14028s. The growth curves of *S.* Typhimurium 14028s carrying pASK-IBA33+ were observed in the presence of varying concentrations of ATc. The optical densities of the cultures were measured periodically.

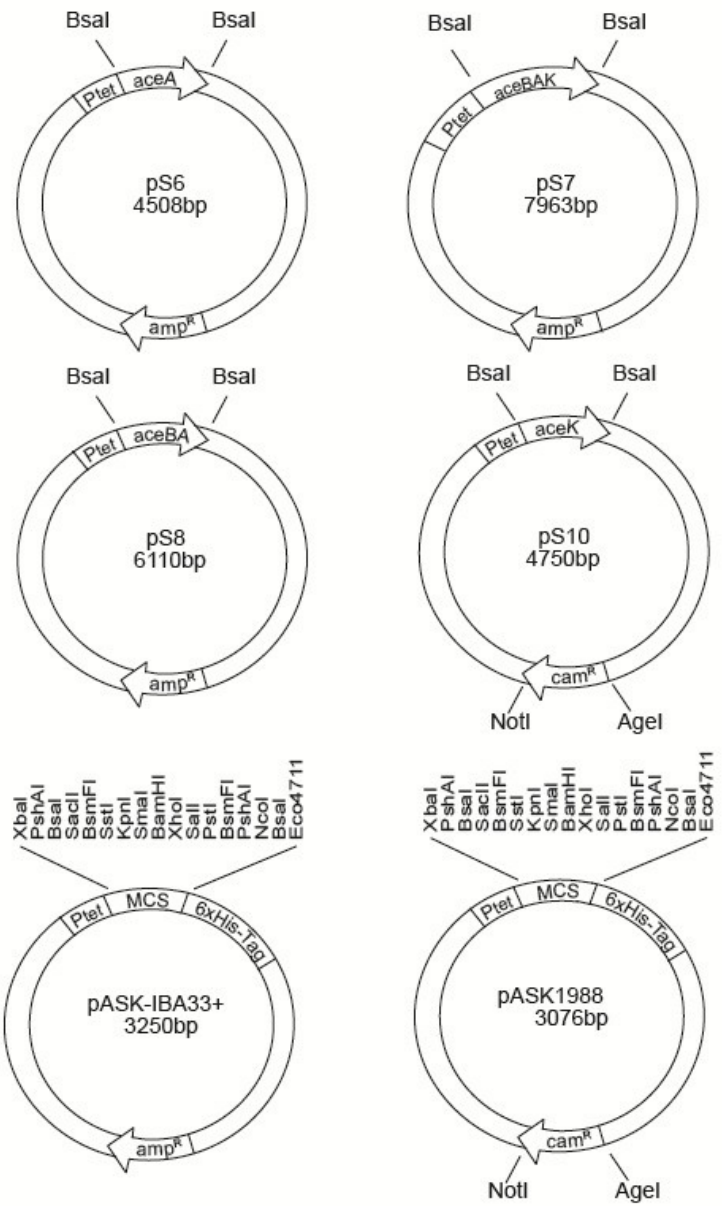

Figure 5: Maps of the expression vectors used in this study.

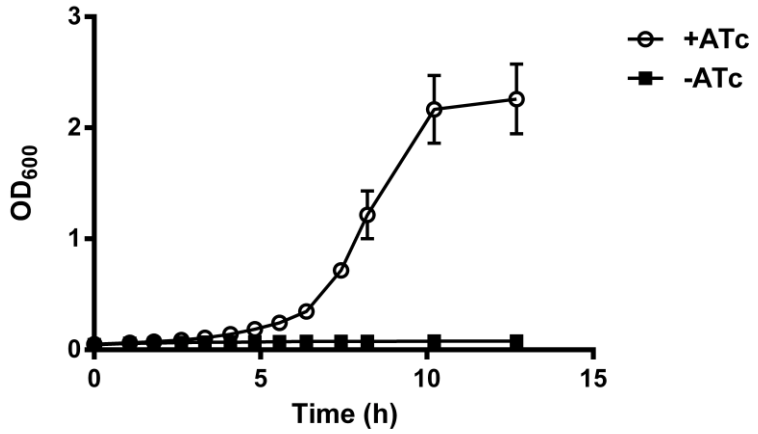

Figure 6: Growth curve of Δ*ppc*(pS8+pS10) in glucose minimal media in the presence and absence of ATc

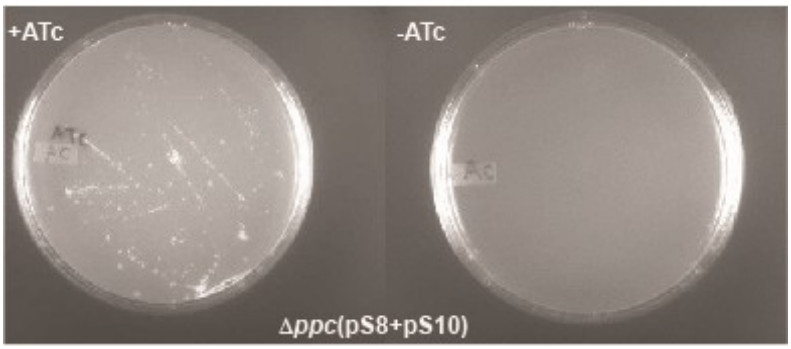

Figure 7: Growth of Δ*ppc*(pS8+pS10) on plates with or without inducer. Plates consisted of glucose minimal media with or without 100 ng/mL of ATc

Table 7: Putative mutations in Δ*ppc*(pS8+pS10) identified by next-generation sequencing

Predicted mutations						
evidence	**seq id**	**position**	**mutation**	**annotation**	**gene**	**description**
RA	NC_016856	215,002	+GA	coding (995/1419 nt)	*pcnB*	poly(A) polymerase I
RA	NC_016856	306,742	C→T	A229T (GCG→ACG)	*STM14_0314*	putative cytoplasmic protein
RA	NC_016856	515,779	+T	intergenic (+36/+13)	*cof/STM14_0542*	putative hydrolase/putative cysteine synthase/cystathionine beta-synthase
RA	NC_016856	1,115,779	+T	intergenic (+49/+39)	*ymbA/STM14_1209*	putative outer membrane protein/hypothetical protein
RA	NC_016856	1,290,524	Δ1 bp	coding (281/300 nt)	*STM14_1424*	prophage RecE
RA	NC_016856	1,328,473	T→A	N625K (AAT→AAA)	*STM14_1478*	side tail fiber protein
RA	NC_016856	1,723,496	T→C	T362A (ACG→GCG)	*STM14_1964*	putative cytoplasmic protein
RA	NC_016856	1,925,863	Δ1 bp	intergenic (-25/+112)	*rnd/tnpA_6*	ribonuclease D/transposase
RA	NC_016856	1,978,116	T→C	S119S (AGT→AGC)	*STM14_2274*	RecE-like protein
RA	NC_016856	2,104,871	+A	coding (270/408 nt)	*STM14_2439*	hypothetical protein
RA	NC_016856	2,391,985	A→T	F42Y (TTT→TAT)	*STM14_2767*	putative cytoplasmic protein
RA	NC_016856	2,480,438	A→G	V206A (GTG→GCG)	*nuoL*	NADH dehydrogenase subunit L

Table 7 continued: Putative mutations in Δ*ppc*(pS8+pS10) identified by next-generation sequencing

evidence	seq id	position	mutation	annotation	gene	description
RA	NC_016856	2,826,322	T→A	Y512N (TAT→AAT)	*STM14_3224*	exodeoxyribonuclease VIII-like protein
RA	NC_016856	2,826,326	T→A	L513Q (CTG→CAG)	*STM14_3224*	exodeoxyribonuclease VIII-like protein
RA	NC_016856	4,122,478	Δ2 bp	coding (53-54/99 nt)	*ilvL*	ilvG operon leader peptide
RA	NC_016856	3,866,453	A→C	T11P (ACC→CCC)	*avtA*	valine--pyruvate transaminase
RA	NC_016856	4,316,301	T→A	E219V (GAA→GTA)	*cytR*	DNA-binding transcriptional regulator CytR
RA	aceK plasmid	4,666	C→T	intergenic (–/–)	–/–	–/–

Table 8: Genes crucial to the *glyA* mutant as predicted by STM_V1.0. (STM2555:*glyA*)

Gene1	Gene2	Minimal Flux of Gene1 KO	Minimal Flux of Gene2 KO	Minimal Flux of Double KO	Priority Score (Difference in Total Minimal Flux)
STM2555	STM2952	131.8802465	141.4283568	148.1784962	6.750139413
STM2555	STM2326	131.8802465	156.7723307	162.6409041	5.868573377
STM2555	STM2316.S	131.8802465	156.7723307	162.6409041	5.868573377
STM2555	STM2323.S	131.8802465	156.7723307	162.6409041	5.868573377
STM2555	STM2320	131.8802465	156.7723307	162.6409041	5.868573377
STM2555	STM2327	131.8802465	156.7723307	162.6409041	5.868573377
STM2555	STM2321	131.8802465	156.7723307	162.6409041	5.868573377
STM2555	STM2324	131.8802465	156.7723307	162.6409041	5.868573377
STM2555	STM2322	131.8802465	156.7723307	162.6409041	5.868573377
STM2555	STM2325	131.8802465	156.7723307	162.6409041	5.868573377
STM2555	STM2328	131.8802465	156.7723307	162.6409041	5.868573377
STM2555	STM2319	131.8802465	156.7723307	162.6409041	5.868573377
STM2555	STM2318	131.8802465	156.7723307	162.6409041	5.868573377
STM2555	STM2317	131.8802465	156.7723307	162.6409041	5.868573377
STM2555	STM0441	131.8802465	150.6967836	156.4392881	5.7425045
STM2555	STM0440	131.8802465	150.6967836	156.4392881	5.7425045
STM2555	STM0443	131.8802465	150.6967836	156.4392881	5.7425045
STM2555	STM0442	131.8802465	150.6967836	156.4392881	5.7425045
STM2555	STM3359	131.8802465	131.9492289	137.6134334	5.664204518
STM2555	STM0733	131.8802465	131.4283848	137.0925914	5.21234488
STM2555	STM0734	131.8802465	131.4283848	137.0925914	5.21234488
STM2555	STM0732	131.8802465	131.4283848	137.0925914	5.21234488
STM2555	STM0735	131.8802465	131.4283848	137.0925914	5.21234488
STM2555	STM0154	131.8802465	137.5146429	142.5886319	5.073989021
STM2555	STM1299	131.8802465	132.838507	137.5243211	4.685814149
STM2555	STM2432	131.8802465	131.3904439	136.1790129	4.298766388
STM2555	STM2431	131.8802465	131.3904439	136.1790129	4.298766388
STM2555	STM0737	131.8802465	130.6590772	135.8008219	3.920575348
STM2555	STM0736	131.8802465	130.6590772	135.8008219	3.920575348
STM2555	STM0739	131.8802465	130.3987993	135.5405444	3.660297844
STM2555	STM0738	131.8802465	130.3987993	135.5405444	3.660297844
STM2555	STM0153	131.8802465	130.9176849	135.3765966	3.496350028
STM2555	STM0152	131.8802465	130.9176849	135.3765966	3.496350028

Table 9: Genes crucial to the *serA* mutant as predicted by STM_V1.0. (STM3062: *serA)*

Gene1	Gene2	Minimal Flux of Gene1 KO	Minimal Flux of Gene2 KO	Minimal Flux of Double KO	Priority Score (Difference in Total Minimal Flux)
STM3062	STM2952	134.0651592	141.4283568	156.0121389	14.58378213
STM3062	STM2326	134.0651592	156.7723307	165.0815902	8.309259448
STM3062	STM2316.S	134.0651592	156.7723307	165.0815902	8.309259448
STM3062	STM2323.S	134.0651592	156.7723307	165.0815902	8.309259448
STM3062	STM2327	134.0651592	156.7723307	165.0815902	8.309259448
STM3062	STM2321	134.0651592	156.7723307	165.0815902	8.309259448
STM3062	STM2324	134.0651592	156.7723307	165.0815902	8.309259448
STM3062	STM2325	134.0651592	156.7723307	165.0815902	8.309259448
STM3062	STM2328	134.0651592	156.7723307	165.0815902	8.309259448
STM3062	STM2318	134.0651592	156.7723307	165.0815902	8.309259448
STM3062	STM2317	134.0651592	156.7723307	165.0815902	8.309259448
STM3062	STM2320	134.0651592	156.7723307	165.0815898	8.309259048
STM3062	STM2322	134.0651592	156.7723307	165.0815898	8.309259048
STM3062	STM2319	134.0651592	156.7723307	165.0815898	8.309259048
STM3062	STM0441	134.0651592	150.6967836	158.9119018	8.21511815
STM3062	STM0440	134.0651592	150.6967836	158.9119018	8.21511815
STM3062	STM0443	134.0651592	150.6967836	158.9119018	8.21511815
STM3062	STM0442	134.0651592	150.6967836	158.9119018	8.21511815
STM3062	STM0154	134.0651592	137.5146429	144.7597069	7.24506402
STM3062	STM3359	134.0651592	131.9492289	140.020256	5.955096814
STM3062	STM1299	134.0651592	132.838507	139.6823841	5.617224862
STM3062	STM0733	134.0651592	131.4283848	139.499412	5.434252755
STM3062	STM0734	134.0651592	131.4283848	139.499412	5.434252755
STM3062	STM0732	134.0651592	131.4283848	139.499412	5.434252755
STM3062	STM0735	134.0651592	131.4283848	139.499412	5.434252755
STM3062	STM3865	134.0651592	235.770206	240.1502709	4.3800649
STM3062	STM3867	134.0651592	235.770206	240.1502709	4.3800649
STM3062	STM3868	134.0651592	235.770206	240.1502709	4.3800649
STM3062	STM3871	134.0651592	235.770206	240.1502705	4.3800645
STM3062	STM3870	134.0651592	235.770206	240.1502705	4.3800645
STM3062	STM3866	134.0651592	235.770206	240.1502705	4.3800645
STM3062	STM3864	134.0651592	235.770206	240.1502705	4.3800645
STM3062	STM3869	134.0651592	235.770206	240.1502705	4.3800645

Table 9 continued: Genes crucial to the *serA* mutant as predicted by STM_V1.0. (STM3062: *sera)*

Gene1	Gene2	Minimal Flux of Gene1 KO	Minimal Flux of Gene2 KO	Minimal Flux of Double KO	Priority Score (Difference in Total Minimal Flux)
STM3062	STM2432	134.0651592	131.3904439	138.3780121	4.312852878
STM3062	STM2431	134.0651592	131.3904439	138.3780121	4.312852878
STM3062	STM0737	134.0651592	130.6590772	138.0459104	3.98075118
STM3062	STM0736	134.0651592	130.6590772	138.0459104	3.98075118
STM3062	STM3069	134.0651592	152.1902247	156.0121389	3.821914205
STM3062	STM1290	134.0651592	152.1902247	156.0121389	3.821914205
STM3062	STM0739	134.0651592	130.3987993	137.7856329	3.720473675
STM3062	STM0738	134.0651592	130.3987993	137.7856329	3.720473675
STM3062	STM1883	134.0651592	127.1176578	137.5597636	3.494604411
STM3062	STM0153	134.0651592	130.9176849	137.4149951	3.349835895
STM3062	STM0152	134.0651592	130.9176849	137.4149951	3.349835895

SUPPLEMENTARY MATERIAL

Table S1: Primers used for generation of kanamycin resistance cassettes

Name	**Sequence 5'->3'**
gltB_KO_Forward	TGCCCGCGCGCCGTCGGTTGGGAGAGCGTCCCGTAGAGCCTGG GGAGGTTCACTGATATG ATTCCGGGGATCCGTCGACC
gltB_KO_Reverse	CGGATCAACGCGCTGCAGGTCGATAAATTGATAAACATTCTGGCT CATTTCAATTCCTTA GTGTAGGCTGGAGCTGCTTC
sucC_KO_Forward	GCCTACAGGTCTAAAGATAACGATTACCTGAAGGATGGACAGAA CACATGAACTTACATG ATTCCGGGGATCCGTCGACC
sucC_KO_Reverse	GGCTACCGGTGAAGCCCTGGCAGATAACCTTGGTATCTTTATTAA TTAAAACGGACATTA GTGTAGGCTGGAGCTGCTTC
ppc_KO_Forward:	CGCTGTGGCATGAAAGAGACAGGGCAATTACATTAAAGATGGGG TGTCTGGGGTCAT ATG ATTCCGGGGATCCGTCGACC
ppc_KO_Reverse:	ACAGCAGTATTTCATGCCGCCCCCACATAACTGCGTGAGAGCGG CTCTCTTTTGGCGTTAGTGTAGGCTGGAGCTGCTTC
mdh_KO_Forward	AAGGTCGCCGCCGCGGAGCAATAGACACTTAGCTAATCATATAAT AAGGAGTTTAGGATG ATTCCGGGGATCCGTCGACC
mdh_KO_Reverse	GGCTTGTTTACAGTCAAAGAAGCCGGAGCAAAAGCCCCGGCATC GGGCAGGAACAGCTTA GTGTAGGCTGGAGCTGCTTC
gdhA_KO_Forward	CATATTCTGATAAAACGCAAATACAACCACATTAATATATAAGAGG TTTTTATATCTATG ATTCCGGGGATCCGTCGACC
gdhA _KO_Reverse	TGCGGAGACAGGCCGTCAGACCGAATAAGCGTAAAGCTATCTGG CCTGACGACGGGATTA GTGTAGGCTGGAGCTGCTTC
serA_KO_Forward	AGGACGGATGCAAATCCACACACAACATCAGATGGCAAAAAAGA CAGGATCGGGGAAATG ATTCCGGGGATCCGTCGACC
serA_KO_Reverse	GAGGCAGGGAAACCAGAGAAAGGATGGGCAGGTCATCTCCTGC CCATTTAGCGGAAATTAGTGTAGGCTGGAGCTGCTTC
lpdA_KO_Forward	GGTGGATGATGGGCGATCAAGTACCCCGGACCGCCGGATACAA ATAAAGAGGTCATGATGATTCCGGGGATCCGTCGACC
lpdA_KO_Reverse	AAAGCGGCTGTAAAGCCGCTTTTTTGTATCGGGTGGCGCATTGC CACCTACAGAAGATTAGTGTAGGCTGGAGCTGCTTC
glyA_KO_Forward	CCCACGGACTGCCTTTTCAGGCACAAATTTTATTGTTAGCTGAGT CAGGAGATGCGGATGATTCCGGGGATCCGTCGACC
glyA_KO_Reverse	GCATAAGTAATGCCCGACAGACGCAGCGCCATCGGGCCATTTTC ACAACACAAGCGCTTAGTGTAGGCTGGAGCTGCTTC

Table S2: Primers used for confirmation of kanamycin resistance cassette

Name	**Sequence 5'->3'**
gltB_con_F	TTTACCAATGCGCAAAGGAC
gltB_con_R	GTACCGGACATTTCCACTCG
sucC_con_F	GTCAGCAAGAGCATCACCTG
sucC_con_R	TACCGTAAGCAATCGCCTGT
ppc_con_F	ACGGGTTTTACGTGGCTTTA
ppc_con_R	ATCGTAGCGCCAAACGTAAC
mdh_con_F	GAACGTTGCTCTCTGGTTGC
mdh_con_R	CGAAGCATTTGCGTAATGTG
gdhA_con_F	TCGCCCCGTTATGAATTTAC
gdhA_con_R	AGCTGATCGAGCAGGCTAAG
serA_con_F	TTCCCGGTATTTTCATCTGC
serA_con_R	GCTATGCTGAGCCCTTATCG
lpdA _con_F	AGCGAAAGCGATAATTCGTG
lpdA _con_R	TTTCGTTATCCTTCGCCATC
glyA_con_F	TCGTCAGACTCTCGTTCAGG
glyA_con_R	GCGATAGTCTGGCGGTAAAC

Table S3: Internal primers used to confirm gene knockout

Name	**Sequence 5'->3'**
gltB_internal_F	TCATCGTAGAAACCGGAAGC
gltB_internal_R	AGTTTGGAGCAGCGGTAAGA
sucC_internal_F	CGCGGTAGTTGACCGTAGTT
sucC_internal_R	GGTTGCCAGACCCATAAAGA
ppc_internal_F	ACTCTTGTTAAGCCGCTGGA
ppc_internal_R	CAGCTTCTCGCCTTTCAGAC
mdh_internal_F	AGGCGCTGGCATTACTTTTA
mdh_internal_R	ACGTTAAACAGGTCGGAACG
gdhA_internal_F	CAGAACGAACTGGACGTTGA
gdhA_internal_R	GTCCACTTTCTCGGCTTTCC
serA_internal_F	GCTGGGGATGCATGTCTATT
serA_internal_R	GCACAAAGCCGGGATATCTA
lpdA_internal_F	CGCATCAGCAAGAAATTCAA
lpdA_internal_R	ATAAAGCCACGGTCGTCAAC
glyA_internal_F	CGGTTCTCAGGCTAACTTCG
glyA_internal_R	AATCATCTTCGGCTTGTGCT

Table S4: Primers for construction of pS1988

Name	**Sequence 5'->3'**
pASK(-)amp_F:	CGGCAGACCGGTTAGGAATTAATGATGTCTCGTTTAG
pASK(-)amp_R:	CGGCAGGCTTAGCTCAATATTATTGAAGCATTTATCAGG
camR_R_pACBSR:	CGGCAGGCTAAGCCAGGAGCTAAGGAAGCTAAAATG
camR_R_pACBSR:	CGGCAGACCGGTAAATTACGCCCCGCCCTG

Table S5: Primers for construction of pS6, pS7, pS8, and pS10

Name	**Sequence 5'->3'**
aceBAK_F	CGGCAGGGTCTCAAATGAATCCACAGGCAACCAC
aceBAK_R	CGGCAGGGTCTCGGCGCTTTACGAAGAGTTCGCCGTAC
aceBA_R	CGGCAAGGTCTCAGCGCTTCAAAACTGCGCTTCTTCGG
aceA_R	CGGCAGAAGCTTTCAAAACTGCGCTTCTTCGGT
aceK_F	CGGCAGGGTCTCGAATGCCGCGTGGCCTGGAATT
pASK-IBA33+_conF	GAGTTATTTTACCACTCCCT
pASK-IBA33+_conF	CGCAGTAGCGGTAAACG

REFERENCES

Badie G., Heithoff D.M., Sinsheimer R.L., Mahan M.J. (2007) “Altered levels of Salmonella DNA adenine methylase are associated with defects in gene expression, motility, flagellar synthesis, and bile resistance in the pathogenic strain 14028 but not in the laboratory strain LT2,” J Bacteriol.189(5): 155

Borthwick A.C., Holms W.H., Nimmo H.G. (1984) “The phosphorylation of *Escherichia coli* isocitrate dehydrogenase in intact cells,” Biochem. J. 222(3):797-804

Boucher H.W., Talbot G.H., Bradley J.S., et al. (2009) “Bad bugs, no drugs; no ESKAPE! An update from the Infectious Diseases Society of America,” Clinical Infectious Disease. *48*;1-12

Chung T., Resnik E., Stueland C., LaPorte D. (1993) “Relative expression of the products of glyoxylate bypass operon: contributions of transcription and translation,” J. Bacteriol. 175(14):4572-5

Cortay J.C., Bleicher F., Rieul C., Reeves H.C., Cozzone A.J. (1988) “Nucleotide sequence and expression of the *aceK* gene coding for isocitrate dehydrogenase kinase/phosphatase in *Escherichia coli*,” J. Bacteriol. 170(1):89

Cozzone A.J., El-Mansi M. (2005) “Control of isocitrate dehydrogenase catalytic activity by protein phosphorylation in *Escherichia coli*,” J. Mol. Microbiol. Biotechnol. 9(3-4):132-46

Cunningham L., Guest J.R. (1998) “Transcription and transcript processing in the sdhCDAB-sucABCD operon of *Escherichia coli*,” Microbiology. 144(8):2113-23

Dabbs E.R. (1982) “The gene forribosomal protein L13, *rplM,* is located near *argR,* at about 70 minutes on the *Escherichia coli* chromosomal linkage map,” J. Bacteriol. 149(2):779

Datsenko K.A., Wanner B.L. (2000) “One-step inactivation of chromosomal genes in Escherichia coli K-12 using PCR products,” Proc Natl Acad Sci. 97(12):6640-5

DeWall C.S., Roberts C., Catella C. (2011) “Antibiotic Resistance in Foodborne Pathogens: Evidence of the Need for a Risk Management Strategy,” Washington, DC: Center for Science in the Public Interest. pp. 1-13

Douce R., Bourguignon J., Neuburger M., Rébeillé F. (2001). “The glycine decarboxylase system: a fascinating complex,” Trends. Plant Sci. *6*: 167–76

Ehrt S., Guo X.V., Hickey C.M., Ryou M., Monteleone M., Riley L.W., Schnappinger D. (2005) “Controlling gene expression in mycobacteria with

anhydrotetracycline and Tet repressor," Nucleic Acids Res. 33(2): e21 doi: 10.1093/nar/gni013

Feist A.M., Herrgard M.J., Thiele I., Reed J.L., Palsson BO (2009). "Reconstruction of biochemical networks in microorganisms," Nature Reviews Microbiology. *7(2)*, 129-143

Folger O., Jerby L., Frezza C., Gottlieb E., Shlomi T. (2011) "Predicting selective drug targets in cancer through metabolic networks," Mol Syst Biol. 7;501 doi: 10.1038/msb.2011.35

Fong S.S., Nanchen A., Palsson B.O., Sauer U. (2006) "Latent pathway activation and increased pathway capacity enable *Escherichia coli* adaptation to loss of key metabolic enzymes," J. Biol. Chem. 281(12):8024-33

Harrison R., Papp B., Pal C., Oliver S.G., Delneri D. (2007) "Plasticity of genetic interactions in metabolic networks of yeast". Proc Natl Acad Sci. 104: 2307–2312.

Holmes M.A., Zadoks R.N. (2011) "Methicillin Resistant S. aureus in Human and Bovine Mastitis," J Mammary Gland Biol Neoplasia. 16(4):373-82

Howard B.J., Keisser J.F. (1994) *Clinical and Pathogenic Microbiology*. 2nd ed. (St. Louis , Mo : Mosby) pp. 383-423

Jarvik T., Smillie C., Groisman E., Ochman H. (2010) "Short-term signatures of evolutionary change in the *Salmonella enterica* Serovar Typhimurium 14028 genome," J Bacteriol. 192(2): 560-567

Kaelin William G. (2005) "The concept of synthetic lethality in the context of anticancer therapy," Nature. *5,* 689-97

Kennedy K., Collignon P. (2010) **"**Colonisation with *Escherichia coli* resistant to 'critically important' antibiotics: a high risk for international travellers," Eur J Clin Microbiol Infect Dis. *12*:1501-1506.

Lee T.S., Krupa R.A., Zhang F., Hajimorad M., Holtz W.J., Prasad N., Lee S.K., Keasling J.D. (2011) "BglBrick vectors and datasheets: A synthetic biology platform for gene expression," J. Biol. Eng. **5:**12 doi:10.1186/1754-1611-5-12

Lewis N.E., Hixson K.K., Conrad T.M., Lerman J.A., Charusanti P., Polpitiya A.D., Adkins J.N., Schramm G., Purvine S.O., Lopez-Ferrer D., Weitz K.K., Eils R., Konig R., Smith R.D., Palsson B.O. (2010) "Omics data from evolved *E. coli* are consistent with computed optimal growth from genome-scale models," Mol. Syst. Biol. doi: 10.1038/msb.2010.47

Locke J.B., Rahawi S., Lamarre J., Mankin A.S., Shaw K.J. (2011) “Zyvox Genetic Environment and Stability of cfr in Methicillin-Resistant Staphylococcus aureus CM05,” Antimicrob. Agents Chemother. 56(1):332-40

Lorca G.L., Ezersky A., Lunin V.V., Walker J.R., Altamentova S., Evdokimova E., Vedadi M., Bochkarev A., Savenchenko A. (2007) “Glyoxylate and pyruvate are antagonistic effectors of the *Escherichia coli* IclR transcriptional regulator,” J. Biol. Chem. 282(22):16476-91

Luinenburg I., Coleman J.R. (1993) “Expression of *Escherichia coli* phosphophenolpyruvate carboxylase in a cyanobacterium,” Plant Physiol. 101(1):121-126

Mark, S., Roberts, T., (1993) “*E. coli* O157:H7 ranks as the fourth most costly foodborne disease,” Food Rev. *16*, 51-59.

McKee J.S., Hlodan R., Nimmo H.G. (1989) “Studies of the phosphorylation of *Escherichia coli* isocitrate dehydrogenase. Recognition of the enzyme by isocitrate dehydrogenase kinase/phosphatase and effects of phosphorylation on its structure and properties,” Biochimie. 71(9-10):1059-64

Mellon M., Benbrook C., Benbrook K. (2001) “Hogging it. Estimates of Antimicrobial Abuse in Livestock,” Cambridge: UCS Publications. pp: 1-3.

Miller E.S., Brenchley J.E. “Cloning and characterization of gdhA, the structural gene for glutamate dehydrogenase of *Salmonella* Typhimurium,” J Bacteriol. *157*: 171–178.

Ong S., Nakase J., Moran G.J, Karras DJ., Kuehnert MJ., Talan DA. (2007) “Antibiotic use for emergency department patients with upper respiratory infections: prescribing practices, patient expectations, and patient satisfaction,” Annals of Emergency Medicine. *3*, 213-220

Orth J.D., Conrad T.M., Na J., Lerman J.A., Nam H., Feist A.M., Palsson B.O. (2011) “A comprehensive genome-scale reconstruction of *Escherichia coli* metabolism,” Mol Syst Biol. 7:535 doi:10.1038/msb.2011.65

Peng L., Arauzo-Bravo M.J., Shimizu K. (2004) “Metabolic flux analysis for a ppc mutant *Escherichia coli* based on 13C-labeling experiments together with enzyme activity assays and intracellular metabolite measurements,” FEMS Microbiol Lett. 235(1):17-23

Reed J.L., Famili I., Thiele I., Palsson, B.Ø. (2006) "Towards multidimensional genome annotation," Nature Reviews Genetics. 7(130)-141

Reed J.L., Patel T.R., Chen K.H., Joyce A.R., Applebee M.K., Herring C.D., Bui

O.T., Knight E.K., Fong S.S., Palsson B.Ø. (2006) "Systems Approach to Refining Genome Annotation," Proc Natl Acad Sci USA. 103(46): 17480-84

Shirley D. (2011) *Project Management for Healthcare.* (Boca Rotan, FL:CRC Press) pp. 199

Sohn S.B., Kim T.Y., Lee J.H., Lee S.Y. (2012) “Genome-scale metabolic model of the fission yeast *Schizosaccharomyces pombe* and the reconciliation of *in silico/in vivo* mutant growth,” BMC Syst. Biol. **6:**49 doi:10.1186/1752-0509-6-49

Sutherland P., McAllister-Henn L. (1985) “Isolation and expression of the *Escherichia coli* gene encoding malate dehydrogenase,” J Bacteriol. 163(3):1074-9

Thiele I., Hyduke D., Steeb B., Fankam G., Allen D., et al. (2011) “A community effort towards a knowledge-based and mathematical model of the human pathogen *Salmonella* Typhimurium LT2,” BMC Sys Bio. 5:8

Varma A., Palsson B.O. (1994) “Metabolic flux balancing: basic concepts, scientific and practical use,” Nat. Biotechnology. **12**:994-998

Zhao G, Winkler M.E. (1996) “A novel alpha-ketoglutarate reductase activity of the serA-encoded 3-phosphoglycerate dehydrogenase of Escherichia coli K-12 and its possible implications for human 2-hydroxyglutaric aciduria,” J. Bacteriol. *178*: 232-239